Author/s:
Ciceri, D;Mason, LR;Harvie, DJE;Perera, JM;Stevens, GW

Title:
Modelling of interfacial mass transfer in microfluidic solvent extraction: Part II. Heterogeneous transport with chemical reaction

Date:
2013-01-01

Citation:
Ciceri, D., Mason, L. R., Harvie, D. J. E., Perera, J. M. & Stevens, G. W. (2013). Modelling of interfacial mass transfer in microfluidic solvent extraction: Part II. Heterogeneous transport with chemical reaction. Microfluidics and Nanofluidics, 14 (1-2), pp.213-224. https://doi.org/10.1007/s10404-012-1039-y.

Persistent Link:
https://hdl.handle.net/11343/282895

Microfluid Nanofluid manuscript No.
(will be inserted by the editor)

Modelling of interfacial mass transfer in microfluidic solvent extraction

Part II. Heterogeneous transport with reaction

Davide Ciceri · Lachlan R. Mason · Dalton J. E. Harvie · Jilska M. Perera · Geoffrey W. Stevens

Received: date / Accepted: date

Abstract The use of a microfluidic device in determining the extraction kinetics of Co^{II} ions by di-(2-ethylhexyl) phosphoric acid (DEHPA) was demonstrated. Experimental data obtained using a Y-Y-shaped microchannel were modelled using a finite volume method. The contributions of diffusion and reaction transport resistances to the overall rate of mass transfer were obtained. A diffusion-controlled transfer assumption could not account for the experimental data, confirming that transport occurs under a mixed reaction-diffusion resistance regime. The reaction rate constant was determined to be $(2.4 \pm 0.6) \times 10^{-10}$ m/s, in good agreement with corresponding Lewis cell measurements from the literature.

Keywords Finite volume simulation · Hydrometallurgy · Kinetics · Liquid/liquid interface · Microfluidics · Solvent extraction

1 Introduction

Chemical reactions in the presence of a liquid/liquid interface are common in analytical, biological and engineering processes (Perera and Stevens 2009). Solvent extraction (SX), a separations technology widely applied in the mineral and pharmaceutical industries, exploits interfacial reactions for the purposes of purification and concentration. The target

D. Ciceri · L. R. Mason · D. J. E. Harvie · J. M. Perera · G. W. Stevens
Department of Chemical and Biomolecular Engineering
The University of Melbourne, Melbourne, VIC 3010, Australia
E-mail: gstevens@unimelb.edu.au

aqueous-phase species is selectively transferred across the aqueous/organic interface under the mediation of an extractant. A typical example of hydrometallurgical SX is the selective transfer of a metal ion using a water-insoluble organophosphorous extractant (Flett 2005), with the reaction considered to occur at the interface (Komasawa and Otake 1983; Stevens et al. 2001).

Overall extraction rates may be governed by a serial combination of both diffusion and reaction transfer resistances. A method of investigating interfacial reaction kinetics is to eliminate the diffusion resistance. Traditional devices such as the Lewis cell (Lewis 1954a,b) use physical mixing or stirring to minimise the bulk diffusion resistance. As the stirring rate is limited by interfacial stability, the diffusion boundary layers remain non-negligible. Unstirred devices such as static transfer cells have also been used to investigate hydrometallurgical SX kinetics. McCulloch et al. (1996) and Warren et al. (2006) respectively investigated the extraction of Cu^{II} ions by 7-(4-ethyl-1-methyloctyl)-8-hydroxyquinoline (Kelex 100) and the extraction of Ni^{II} by 2-hydroxy-5-nonylacetophenone oxime (LIX 84). However, in order to achieve reaction-controlled conditions, the reactants were restricted to low concentrations. High solute concentrations are important in hydrometallurgical applications; cobalt ion concentrations in extracted liquors, for example, can be as high as 0.85 M (Lo et al. 1983). Despite the use of a variety of bulk-scale devices, such as the AKUFVE apparatus (Rydberg 1969), the rotating diffusion cell (Albery et al. 1976) and the growing drop technique (Hughes and Zhu 1985), the reaction mechanism of many hydrometallurgical extractions is not well understood (Ciceri et al. 2011b).

SX can benefit from advances in microfluidic technology (Aota et al. 2009; Kuban et al. 2003; Priest et al. 2011; Tokeshi et al. 2000), allowing increases in system throughput-to-volume ratios and a significant reduction in the quantities of chemicals used (Ciceri et al. 2011b). A greater range of chemicals can potentially be processed, including species that are otherwise difficult to handle by conventional dispersive methods due to the formation of stabilised emulsions (Priest et al. 2011). Microfluidic solvent extraction (μSX) takes advantage of the distinguishing characteristics inherently related to the micro scale, including large specific interfacial areas and both short diffusion length and time scales. These properties enable extractions to take place without mechanical stirring, mixing, or shaking (Tokeshi et al. 2000).

Relevant heterogeneous extraction experiments, in which two immiscible fluids are brought together inside a microchannel, were detailed in Mason et al. (2012), hereafter

referred to as Part I. The μSX of metal ions in water/oil systems has been reported. Kim et al. (2000) studied the extraction of Al^{III} by 2,2′-dihydroxyazobenzene (DHBA) in a water/butanol system. Mass transport was modelled using a one-dimensional diffusion equation in which interfacial transfer resistances were neglected. Maruyama et al. (2004) reported on the extraction and back-extraction of Y^{III} and Zn^{II} by 2-ethylhexyl phosphonic acid mono-2-ethylhexyl ester (PC-88A) in a three layer water/*n*-heptane/water system. Diffusion was determined to be the rate controlling mechanism and was modelled using a one-dimensional diffusion equation. Hotokezaka et al. (2005) studied the extraction of U^{IV} by tri-*n*-butyl-phosphate (TBP) in a water/*n*-dodecane system. The microfluidic extraction efficiency was observed to increase in comparison to the corresponding traditional bulk extraction, however no kinetic model was proposed. Nagai et al. (2009) used a fluorescence method to study the extraction of Ag^{I} by a crown ether (HTCO) and eosin Y in a water/1,2-dichloroethane system. An extraction mechanism was proposed and the rate controlling transport mechanism was found to be diffusion. Morita et al. (2010) studied the extraction of Cu^{II} by potassium dioctyldithiocarbamate in a water/cyclohexane system. The system was modelled assuming a pseudo-first-order transfer mechanism in the presence of excess extractant and an apparent kinetic constant was determined. Nichols et al. (2011) used a droplet-based microfluidic system to investigate the reactive transfer of lanthanides across a water/*n*-dodecane interface. A first-order decay equation was used to determine interfacial transfer rate constants. Though not focusing on metal ions, Žnidaršič-Plazl and Plazl (2009) studied a lipase-catalysed enzymatic reaction occurring at a water/*n*-hexane interface. A three-dimensional finite difference model accounting for convection, diffusion and an interfacial reaction was used for kinetic parameter determination.

A typical example of reactive hydrometallurgical SX is the extraction of Co^{II} ions by di-(2-ethylhexyl) phosphoric acid (DEHPA). Equilibrium and kinetic studies for this process are summarised in Tables 1 and 2 respectively. There is disagreement among the results for the reaction equilibrium constant K_{eq} and the controlling transport resistance. When reaction-controlled mass transfer has been concluded, there has been disagreement concerning the reaction mechanism used in the interpretation of the kinetic data. The DEHPA extractant (denoted HL) is known to exist as a dimer $(HL)_2$ in both aliphatic and aromatic solvents (Biswas et al. 2003; Danesi et al. 1985) and the extraction reaction is generally considered to follow the stoichiometry (Ciceri et al. 2011b; Komasawa et al. 1981; Komasawa and Otake 1983)

$$\mathrm{Co^{II}_{(aq)}} + 2\,(\mathrm{HL})_{2\,(org)} \rightleftharpoons \mathrm{CoL_2(HL)_{2\,(org)}} + 2\,\mathrm{H^+_{(aq)}}\,, \tag{1}$$

with an equilibrium constant K_{eq} given by

$$K_{eq} = \frac{[\mathrm{CoL_2(HL)_2}]_{eq}[\mathrm{H^+}]^2_{eq}}{[\mathrm{Co^{II}}]_{eq}[(\mathrm{HL})_2]^2_{eq}}\,. \tag{2}$$

The extraction equilibrium depends on several concentration-dependent factors including the aqueous metal ion speciation, aggregation and activity of the extractant in the organic phase (Danesi and Vandegrift 1981), ionic strength and the presence of buffers such as the acetic acid/sodium acetate couple ($\mathrm{AcH/Ac^-}$). An alternative stoichiometry to Eq. 1, in which three molecules of $(\mathrm{HL})_2$ are required to extract one $\mathrm{Co^{II}}$ ion, has been proposed (Cianetti and Danesi 1983; Simonin et al. 1991). Beneitez et al. (1985) investigated the role of sodium acetate in the extraction equilibrium, concluding that an extracted species of the type $(\mathrm{CoAc_2})\mathrm{L_2(HL)_4}$ must exist in the organic phase. Van de Voorde et al. (2005) found no evidence proving that the acetate ion has an active role of in the formation of the $\mathrm{CoL_2(HL)_2}$ complex. Wasan et al. (1984) showed that the extraction kinetics are strongly accelerated by ligands such as acetate. Using a Lewis cell, the average transfer coefficient was shown to increase approximately 65-fold in the presence of sodium acetate. The formation of a kinetically labile complex of the type $\mathrm{Co(H_2O)_4(Ac)_2}$ was hypothesised in explaining the kinetic data.

The extraction mechanism of $\mathrm{Co^{II}}$ by DEHPA has been the subject of controversy. Some studies have considered the reaction to be purely interfacial (Cianetti and Danesi 1983; Komasawa and Otake 1983) due to the low solubility of DEHPA in the aqueous phase (Sella and Bauer 1988). Using an ARMOLLEX apparatus, Cianetti and Danesi (1983) proposed a model of mass transfer with chemical reaction (MTWCR), where the interfacial reaction follows the mechanism:

$$\mathrm{Co^{II}_{(aq)}} + 2\mathrm{HL_{(int)}} \underset{k_b}{\overset{k_f}{\rightleftharpoons}} \mathrm{CoL_{2\,(int)}} + 2\,\mathrm{H^+_{(aq)}} \tag{3}$$

$$\mathrm{CoL_{2\,(int)}} + 3\,(\mathrm{HL})_{2\,(org)} \underset{k'_b}{\overset{k'_f}{\rightleftharpoons}} \mathrm{CoL_2(HL)_{4\,(org)}} + 2\,\mathrm{HL_{(int)}} \tag{4}$$

In the first step (Eq. 3), a reaction between Co^{II} ions and an interfacial HL species leads to the formation of an interfacial CoL_2 complex. In the second step (Eq. 4), the complex reacts with bulk organic-phase dimer $(HL)_2$. Eq. 4 involves the elementary reaction of four molecules, an event that is physically unlikely. Using a Lewis cell, Komasawa and Otake (1983) also proposed an interfacial mechanism:

$$\mathrm{Co(H_2O)_{6\,(aq)}^{2+} + (HL)_{2\,(int)} \underset{k_{-1}}{\overset{k_1}{\rightleftharpoons}} Co(H_2O)_4^{2+}{\cdot}2L_{(int)}^{-} + 2H_3O_{(aq)}^{+}} \tag{5}$$

$$\mathrm{Co(H_2O)_4^{2+}{\cdot}2L_{(int)}^{-} + (HL)_{2\,(int)} \underset{k_{-2}}{\overset{k_2}{\rightleftharpoons}} CoL_2(HL)_{2\,(org)} + 4H_2O_{(aq)}} \tag{6}$$

The first step (Eq. 5) involves an outer-sphere association between the $Co(H_2O)_6^{2+}$ aquo complex and an interfacial $(HL)_2$ ligand. In the rate-determining step (Eq. 6), a second $(HL)_2$ ligand enters into the primary coordination sphere, replacing the outgoing water molecules. The mechanism assumes that Co^{II} at the interface obeys the same Eigen mechanism as in the bulk aqueous phase (Eigen 1963; Cotton and Wilkinson 1988; Cianetti and Danesi 1983; Komasawa and Otake 1983). The concentration of interfacial $(HL)_2$ was assumed to be proportional to that in the bulk phase. Dreisinger and Cooper (1986) have also considered the existence of interfacial $(HL)_2$, however this species remains hypothetical.

Other studies, in contrast, have accounted for interfacial partitioning of DEHPA by proposing a reaction occurring within a thin layer in the aqueous phase (Hughes and Zhu 1985; Dreisinger and Cooper 1989). Using a growing-drop apparatus at industrial (high) concentrations, Hughes and Zhu (1985) proposed a MTWCR model with the rate-controlling steps:

$$\mathrm{Co_{(aq)}^{II} + L_{(aq)}^{-} \underset{k_b}{\overset{k_f}{\rightleftharpoons}} CoL_{(aq)}^{+}} \tag{7}$$

$$\mathrm{CoL_{(aq)}^{+} + L_{(aq)}^{-} \underset{k'_b}{\overset{k'_f}{\rightleftharpoons}} CoL_{2\,(aq)}} \tag{8}$$

Dreisinger and Cooper (1989) adopted the same MTWCR model using a rotating diffusion cell. An additional reaction involving an aqueous dimer was also included:

$$\mathrm{Co_{(aq)}^{II} + HL_{2\,(aq)}^{-} \underset{k_b}{\overset{k_f}{\rightleftharpoons}} CoHL_{2\,(aq)}^{+}}\,. \tag{9}$$

Table 1: Literature values of the equilibrium constant K_{eq} for the extraction of Co^{II} by DEHPA determined under various experimental conditions

Source	Solvent	K_{eq}	T (K)	Buffer	I (mM)
Grimm and Kolařík (1974)	dodecane	3.9×10^{-5}	–	$(Na,H)NO_3$	1000
Cianetti and Danesi (1983) [a]	dodecane	6.3×10^{-3}	–	$(H,K)NO_3$	100
Present study	decane	$(2.7 \pm 0.5) \times 10^{-5}$	293	AcH/Ac^-	100
Komasawa et al. (1981)	heptane	4.0×10^{-5}	298	$(Na,H)NO_3$	500
Ibid.	heptane	6.0×10^{-5}	298	AcH/Ac^-	–
Komasawa and Otake (1983)	heptane	1.8×10^{-5}	298	AcH/Ac^-	–
de Voorde et al. (2006)	hexane	1.5×10^{-6}	–	AcH/Ac^-	–
Huang and Tsai (1990)	kerosene	3.84×10^{-6}	298	$(Na,H)SO_4$	500
Komasawa et al. (1981)	toluene	4.5×10^{-6}	298	$(Na,H)NO_3$	500
Ibid.	toluene	6.5×10^{-6}	298	AcH/Ac^-	–
Komasawa and Otake (1983)	toluene	2.8×10^{-6}	298	AcH/Ac^-	–

[a] The authors reported a stoichiometry of $3\,(HL)_2 : 1\,Co^{II}$

The existence of the aqueous dimer HL_2^- is uncertain since it is generally assumed that only the monomeric HL is capable of being distributed across the interface (Biswas et al. 2003; Sella and Bauer 1988).

In the present study, the Y-Y-shaped microfluidic cell is introduced as an innovative method for kinetic determinations. The extraction of Co^{II} by DEHPA in an AcH/Ac^- buffer was chosen as extraction system. Computational fluid dynamics (CFD) was used to simulate the experimental data of Ciceri et al. (2011b). A sensitivity study was used to investigate the transport regime of the extraction assuming the two-step interfacial reaction mechanism of Komasawa and Otake (1983) (Eqs. 5 and 6). The reaction rate constant was treated as an unknown fitting parameter and determined through regression to experimental results. Hence, a method for obtaining kinetic information of hydrometallurgical extraction processes based on μSX experiments was demonstrated. Additional experimental results were undertaken investigating the effect of higher extractant concentration on the kinetics.

2 Experimental method

2.1 Chemicals and Materials

Di-(2-ethylhexyl) phosphoric acid (99.4%, Tokyo Chemical Industry, lot 26OVA), acetic acid glacial (analytical grade, Univar), sodium acetate anhydrous (analytical grade, Chem-Supply), and cobalt(II) chloride hexahydrate (Sigma-Aldrich) were all used as received. Decane (99% ReagentPlus®, Sigma-Aldrich) was used without further purification. All

Table 2: Overview of experimental conditions of kinetic literature studies on the extraction of Co^{II} by DEHPA

Technique	T (K)	Solvent	$[Co^{II}]$ (mM)	$[(HL)_2]$ (mM)	Mechanism considered
Lewis cell [a]	298	kerosene	68–200	100–500	Interfacial reaction with a diffusion contribution
Lewis cell [b]	–	Shellsol LX154™/TBP	33.9	150 (10% v/v)	Diffusion
Lewis cell [c]	–	Shellsol LX154™/TBP	33.4–34.4	150 (10% v/v)	Diffusion
Lewis cell [d]	298	*n*-heptane	1.0–10	1.5–80	Interfacial reaction
Lewis cell [d]	298	toluene	1.0–10	1.5–80	Interfacial reaction
ARMOLLEX [e]	298	*n*-dodecane	–	2–300	Interfactial reaction or diffusion
Lewis cell [f]	–	kerosene/TBP	31.4–35.6	150 (10% v/v)	Interfacial reaction
Lewis cell [f]	–	kerosene	35.6–41.1	300 (20% v/v)	Interfacial reaction
Growing drop cell [g]	298	*n*-heptane	93.8–100	286–572	Aqueous mechanism[#]
Rotating cell [h]	298/333	*n*-heptane	1.0–200	1–200	Aqueous mechanism[#]
Rotating cell [i]	297	*n*-dodecane	–	200	Interfacial reaction
Permeation cell [j]	303	kerosene	0.2–4.7	20–200	Interfacial reaction
Rotating cell [k]	297	*n*-dodecane	1.0	200	Interfacial reaction
Rotating cell [l]	295	*n*-dodecane	2.0×10^{-5}	20–200	Aqueous mechanism[#]
Present study	293	*n*-decane	5	5–10	Interfacial reaction

[#]Reaction in a thin layer near the interface on the aqueous side

[a] Brisk and McManamey (1969)
[b] Golding et al. (1977)
[c] Golding and Saleh (1980)
[d] Komasawa and Otake (1983)
[e] Cianetti and Danesi (1983)
[f] Golding and Pushparajah (1985)
[g] Hughes and Zhu (1985)
[h] Dreisinger and Cooper (1989)
[i] Simonin et al. (1991)
[j] Juang and Jiang (1994)
[k] Simonin (1996)
[l] Simonin et al. (2003)

aqueous solutions were made up in distilled water (milli-Q®) with an electrical resistivity of less than 18.2 Ω M cm. Water and decane were pre-saturated by contact under shaking for 24 hours.

2.2 Extraction procedure

The Y-Y-shaped microchannel used (ICC-DY05G, Institute of Microchemical Technology Co., Ltd.) has been described previously (Ciceri et al. 2011a,b; Nishi et al. 2010, 2011) and a schematic given in Part I. To achieve a stable water/oil interface the glass surface of the microchannel was selectively coated with silane as per Ciceri et al. (2011b). The extraction procedure and experimental apparatus have also been described previously (Ciceri et al. 2011a,b). Two plastic syringes containing respectively a buffered solution of Co^{II} and a decane solution of DEHPA were placed in two independent syringe pumps, and then the liquids pumped into the microchannel. The flow rates of both the aqueous and organic streams were progressively increased, with the purpose of generating a series of outlet concentrations

for different contact times between the phases. In order to maintain the water/oil interface at the microchannel centreline, the aqueous and organic flow rates were adjusted and were not equal. The extraction of Co^{II} ions by DEHPA proceeded along the water/decane interface before the organic and aqueous streams became separated at the Y-outlet. The pH of the aqueous solution was fully buffered. Organic phase samples were collected at the outlet and analysed spectrophotometrically *ex situ* ($\varepsilon_{CoL_2(HL)_2} = 247 \pm 2\,M^{-1}\,cm^{-1}$ at 627 nm (Ciceri et al. 2011b)). All experiments were conducted at a temperature of 293 K.

2.3 Equilibrium constant determination

The equilibrium constant K_{eq} was determined using classic shake tests. Co^{II} chloride solutions were prepared by means of an AcH/Ac^- buffer with initial pH = 4.4. The buffered Co^{II} solution had an initial total ionic strength of $I = 100$ mM. Extractant solutions were prepared at different concentrations by dissolving a known amount of DEHPA in decane. Equal volumes (20 mL) of aqueous and organic solution were contacted under shaking for 24 hours at 293 K. The shaker (Thermoline Scientific 590) allowed a temperature control of ± 0.1 K. Flasks were let to rest and the aqueous and organic phases were separated. The organic phase was analysed with a UV-Vis spectrophotometer (Varian, Cary, 1E). The acidity of the aqueous phase was determined with a pH meter (Cyberscan 510). The pH was fully buffered. The remaining species concentrations were determined using mass balance calculations.

3 Theoretical background

3.1 Reaction mechanism

The partitioning of DEHPA across water/oil interfaces has been investigated previously (Komasawa et al. 1981; Sella and Bauer 1988; Biswas et al. 2003), with general agreement on the values of dimerisation constant K_2 and monomeric distribution constant K_d. Based on the parameter values of Komasawa et al. (1981) ($K_2 = 32\,mM^{-1}$, $K_d = 1580$), the equilibrium aqueous-phase concentration of HL was determined to be between $(2.5–3.5)\times10^{-3}$ mol% for an initial organic-phase $(HL)_2$ concentration in the range 5–10 mM. Given this low aqueous-phase concentration, the interfacial mechanism of Komasawa and Otake (1983)

(Eqs. 5 and 6) has been used in all simulations. The priority of the present study is to demonstrate that kinetic data can be collected in the Y-Y-shaped microfluidic cell, but not to establish a universal extraction mechanism for the system. Hence, the alternative aqueous-phase mechanistic framework (Hughes and Zhu 1985; Dreisinger and Cooper 1989) has not been investigated. Reactions due to organic-phase impurities and stripping of the silane microchannel coating were assumed to be negligible.

3.2 Numerical simulation

CFD techniques were used to describe both diffusion throughout the liquid volumes and the reaction of species at the interface. A finite volume algorithm, *arb* (Harvie 2012), was used to simulate literature data (Ciceri et al. 2011b) and new experimental data. Model equations, treatment of the interface and boundary conditions (that are not specific to the reactions occurring at the interface) have been discussed in Part I.

3.2.1 Momentum balance equations

As per Part I, the solvent velocity was found by solving the incompressible continuity and steady-state Navier-Stokes equations in conservative form. Gravitational effects were assumed negligible ($Bo = \Delta\rho g D_\mathrm{h}^2/\gamma \ll 1$ for all cases considered). Two notable assumptions were used to simplify the computations: (i) the interface was assumed to be flat and (ii) the velocity profile in both streams was assumed to be fully developed. These allowed a two-dimensional solution of the Navier-Stokes equations to be extruded into the third dimension. Boundary conditions were identical to those used in Part I: (i) the fluid velocity and momentum flux were assumed to be continuous over the two-phase interface and (ii) a no-slip velocity condition was assumed on the walls. The flow rate of each phase was set through phase-specific x-direction pressure gradients such that the corresponding experimental flow rates were matched.

3.2.2 Species balance equations

The local species concentrations c_j were determined using the steady-state advection-diffusion equation

$$\nabla \cdot (c_j \mathbf{u} - \mathscr{D}_{j,i} \nabla c_j) = 0\,, \tag{10}$$

where $\mathbf{u}$ is the fluid velocity and $\mathscr{D}_{j,i}$ is the diffusivity of species j in phase i. Here $j = 1,2,3$ respectively for the species Co^{II}, $(HL)_2$ and $CoL_2(HL)_2$, and $i = 1,2$ for the aqueous and organic phase respectively. An infinitely thin two-phase interface was assumed, with the extraction reaction occurring according to the stoichiometry of Eq. 1. The inner-sphere water rate exchange for Co^{II} is of order $10^6\,s^{-1}$ (Cotton and Wilkinson 1988; Hughes and Zhu 1985), suggesting that dynamic equilibrium is reached instantaneously for Eq. 5. Hence, the dehydration process (Eq. 6) was assumed to be the rate limiting step, allowing the reaction rate to be expressed as (Komasawa and Otake 1983):

$$R = k_2 K_1 \left(\frac{[Co^{II}][(HL)_2]^2}{[H^+]^2} - \frac{k_{-2}}{k_2 K_1} [CoL_2(HL)_2] \right), \tag{11}$$

where $R\,(\mathrm{mol/m^2\,s})$ is the flux of the $CoL_2(HL)_2$ complex generated at the interface. The mass-action constant k_2K_1/k_{-2} has been shown (Komasawa and Otake 1983) to be approximately equal to the equilibrium extraction constant K_{eq}:

$$K_{eq} \simeq \frac{k_2 K_1}{k_{-2}}\,. \tag{12}$$

This is consistent with Eq. 6 reaching dynamic equilibrium. A device-independent (Nichols et al. 2011) rate constant parameter A was defined by

$$A \stackrel{\text{def}}{=} k_2 K_1\,, \tag{13}$$

allowing Eq. 11 to be rewritten as

$$R = A \left(\frac{[Co^{II}][(HL)_2]^2}{[H^+]^2} - \frac{1}{K_{eq}} [CoL_2(HL)_2] \right). \tag{14}$$

Eq. 14 was then used to impose a conservation of mass boundary condition across the interface via flux matching:

$$-\mathscr{D}_{j,i} \frac{\partial c_j}{\partial y}\bigg|_{y \to y_{int}} = (-1)^i \nu_j R\,, \tag{15}$$

where y_{int} is the y-coordinate of the interface and ν_j is the stoichiometric number of each species in Eq. 1. This assumes that no mass transfer of species across the interface occurs, as confirmed by the high value of partition coefficient (K_d) of DEHPA (Komasawa et al. 1981). Expanding Eq. 15 gives

$$-\mathscr{D}_{\mathrm{Co^{II}},1}\left.\frac{\partial[\mathrm{Co^{II}}]}{\partial y}\right|_{y\to y_{\mathrm{int}}^{-}} = R \tag{16}$$

$$-\mathscr{D}_{(\mathrm{HL})_2,2}\left.\frac{\partial[(\mathrm{HL})_2]}{\partial y}\right|_{y\to y_{\mathrm{int}}^{+}} = -2R \tag{17}$$

$$-\mathscr{D}_{\mathrm{CoL_2(HL)_2},2}\left.\frac{\partial[\mathrm{CoL_2(HL)_2}]}{\partial y}\right|_{y\to y_{\mathrm{int}}^{+}} = R \tag{18}$$

If the rate constant A approaches infinity, the simulation describes a system where reaction kinetics are instantaneous (diffusion is the controlling transport resistance).

All further concentration boundary conditions were identical to those used in Part I: a no-flux condition was assumed on all walls and the outlet solute concentration was assumed to be fully developed. Physical properties used are shown in Table 3.

Properties of the various meshes used for resolution independence testing purposes were also given in Part 1. The difference between results obtained using the most coarse and fine mesh was found to be less than 1%.

Table 3: Physical properties used for simulation of experimental data. Reference conditions are 1 atm and 293 K

	Aqueous	Organic
$\mathscr{D}_{\mathrm{Co^{II}},i}$ ($\mathrm{m^2/s}$)	8.25×10^{-10} [a]	–
$\mathscr{D}_{(\mathrm{HL})_2,i}$ ($\mathrm{m^2/s}$)	–	5.0×10^{-10} [b]
$\mathscr{D}_{\mathrm{CoL_2(HL)_2},i}$ ($\mathrm{m^2/s}$)	–	3.2×10^{-10} [c]
μ_i (Pa s)	1.0×10^{-3}	9.1×10^{-4} [d]
ρ_i ($\mathrm{kg/m^3}$)	998[e]	732[d]
D_{h} (μm)	54	

[a] Dreisinger and Cooper (1986)
[b] Wilke-Chang equation (Perry and Green 2007; Wilke and Chang 1955) with $V_{\mathrm{N}} = 846\,\mathrm{m^3/kmol}$ (MacLean and Dreisinger 1993) where V_{N} is the normal molar volume of the solute
[c] Nishi et al. (2011)
[d] Yaws (2003)
[d] Perry and Green (2007)

4 Results and discussion

4.1 Experimental determination of equilibrium constant

Shake test data were used to determine the equilibrium constant K_{eq} for the experimental conditions considered presently. As shown in Figure 1, K_{eq} was determined to be $K_{eq} = (2.7 \pm 0.5) \times 10^{-5}$ via regression to Eq. 2. This value is of similar magnitude to the experimental literature values obtained using aliphatic solvents shown in Table 1.

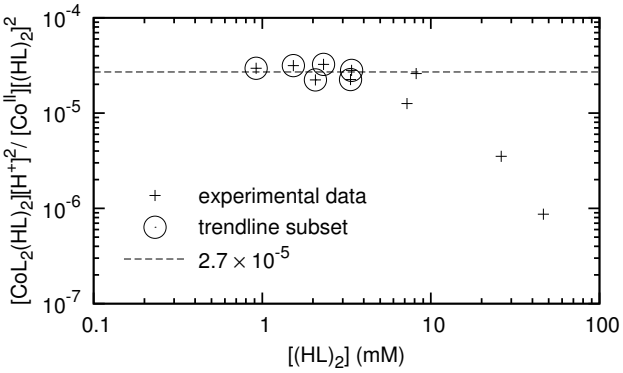

Fig. 1: Determination of the equilibrium constant K_{eq} based on Eqs. 1 and 2. $[(HL)_2]_0$ between 1 and 10 mM; $[Co^{II}]_0 = 5$ mM; $I = 100$ mM; $pH_0 = 4.4$; $T = 293$ K

4.2 Reaction rate constant determination

The reaction rate constant was determined using a least-squares fit to the experimental data of Ciceri et al. (2011b). A residual sum of squares (RSS) was defined by

$$\mathrm{RSS} = \sum_{n=1}^{N} (\bar{c}_{\mathrm{exp},n} - \bar{c}_{\mathrm{sim},n})^2 , \tag{19}$$

where $\bar{c}_{\mathrm{exp},n}$ and $\bar{c}_{\mathrm{sim},n}$ are the velocity-averaged outlet concentrations of $CoL_2(HL)_2$ for the nth set of corresponding experimental and simulation data points.

The error bounds on the rate constant were determined by assuming an error on each component quantity as shown in Table 4. A $\pm 10\%$ error was assumed for all diffusivity values. In order to determine the lower bound of the rate constant A, a set of simulations was

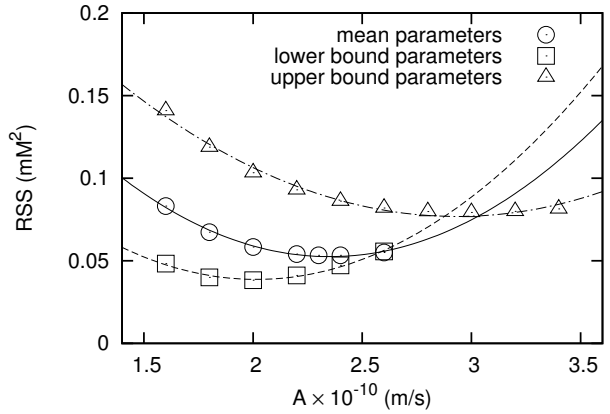

Fig. 2: Comparison of results with lower bound, mean, and upper bound parameters for determining the error bounds of the rate constant A. From the quadratic trendlines shown, a value of $A_{\text{opt}} = (2.4 \pm 0.6) \times 10^{-10}$ m/s was determined. RSS is defined in Eq. 19

undertaken using the lower bound values of both K_{eq} and all diffusivities (denoted as 'lower bound parameters' in Figure 2). Similarly, the upper bounds on all parameters were used to estimate the upper bound on A (denoted as 'upper bound parameters' in Figure 2). Quadratic trend lines were then used to quantitatively determine the error bounds of the optimised rate constant to be $A_{\text{opt}} = (2.4 \pm 0.6) \times 10^{-10}$ m/s. This value agrees (within the error) with that of $A = 1.8 \times 10^{-10}$ m/s obtained experimentally using a Lewis cell device (Komasawa and Otake 1983) and was used in all subsequent simulations. A comparison between simulation results and the experimental data of Ciceri et al. (2011b) is shown in Table 5.

Table 4: Component error bounds assumed in the determination of the total error bound on the rate constant A

	lower bound	mean	upper bound
$\mathscr{D}_{\text{Co}^{\text{II}},\text{aq}}$ ($\times 10^{-10}$ m^2/s) [a]	7.43	8.25	9.08
$\mathscr{D}_{(\text{HL})_2,\text{org}}$ ($\times 10^{-10}$ m^2/s)	4.50	5.00	5.50
$\mathscr{D}_{\text{CoL}_2(\text{HL})_2,\text{org}}$ ($\times 10^{-10}$ m^2/s)	2.90	3.20	3.50
K_{eq} ($\times 10^{-5}$)	2.2	2.7	3.2

[a] A $\pm$10% error was assumed for all diffusivity values

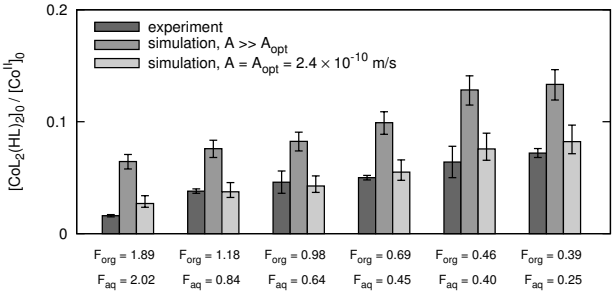

(a) pH = 4.6

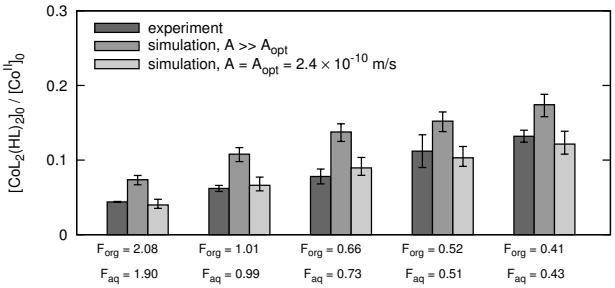

(b) pH = 4.8

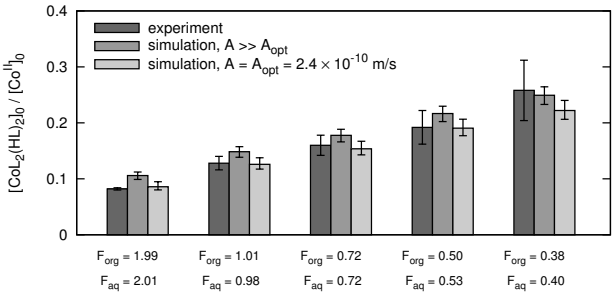

(c) pH = 5.4

Fig. 3: Comparison of simulation results with experimental data (Ciceri et al. 2011b) for the cases of diffusion-controlled transfer resistance ($A \gg A_{\text{opt}}$) and mixed reaction-diffusion resistance ($A = A_{\text{opt}} = 2.4 \times 10^{-10}$ m/s). All flow rates in mL/hr

4.3 Extraction regime

Two mass transfer regimes can typically occur in the extraction system. In a 'diffusion-controlled' regime, reaction of the species takes place on a time scale smaller than that of diffusive transport to the interface. Hence, diffusion is the rate-limiting transport process. In

a ‘reaction-controlled’ regime, it is the reaction rate that limits mass transport. When the diffusion and reaction rates are of similar magnitude, a ‘mixed reaction-diffusion’ regime may exist. Here, it is demonstrated that a diffusion-controlled regime cannot account for the experimental data.

To simulate a diffusion-controlled transfer condition, the reaction rate constant was increased by ten orders of magnitude. Subsequent simulations showed that the outlet product concentration became independent of any further increase in A, indicating that these concentrations ($\bar{c}_{\mathrm{A}\gg\mathrm{A}_{\mathrm{opt}}}$) were equivalent to those obtained under diffusion-controlled conditions. Figure 3 shows outlet concentration results for these diffusion-controlled simulations, as well as simulations using the optimised rate constant obtained in Section 4.2. The diffusion-only simulations overestimate the experimental data for all pH values used. In contrast, the mixed reaction-diffusion simulations are in good agreement with the experimental values.

The simulation error bars in Figure 3 were determined using the lower bound and upper bound parameters of Table 4 as inputs for the physical parameters. For the mixed reaction-diffusion case, the error bounds on the rate constant A_{opt} were also used (see Figure 2). In Figures 3a and 3b, the experimental and diffusion-controlled simulation error bars do not overlap. Hence, attribution of the high diffusion-controlled simulation deviation to uncertainty in the physical parameter values used is extremely unlikely.

To show that the kinetics influence the transfer rate, a Mean Absolute Percentage Error (MAPE) was determined using

$$\mathrm{MAPE}_{\mathrm{exp}} = \frac{1}{N}\sum_{n=1}^{N}\left|\frac{\bar{c}_{\mathrm{exp},n}-\bar{c}_{\mathrm{sim},n}}{\bar{c}_{\mathrm{exp},n}}\right|\times 100\%\,, \tag{20}$$

where N is the number of data points considered and the experimental velocity-averaged outlet concentration $\bar{c}_{\mathrm{exp}}$ has been used as a reference for comparison. Figure 4 shows the values of $\mathrm{MAPE}_{\mathrm{exp}}$ obtained for simulations of the experimental data of Ciceri et al. (2011b). Two key observations can be made from Figure 4:

(i) the $\mathrm{MAPE}_{\mathrm{exp}}$ values for the mixed reaction-diffusion case are lower than the diffusion-controlled case for all pH values, indicating that both kinetic and diffusional resistances are important for this system

(ii) the $\mathrm{MAPE}_{\mathrm{exp}}$ value for the diffusion-controlled simulations decreases with increasing pH, consistent with an increase in the reaction rate according to Eq. 14. A faster reaction

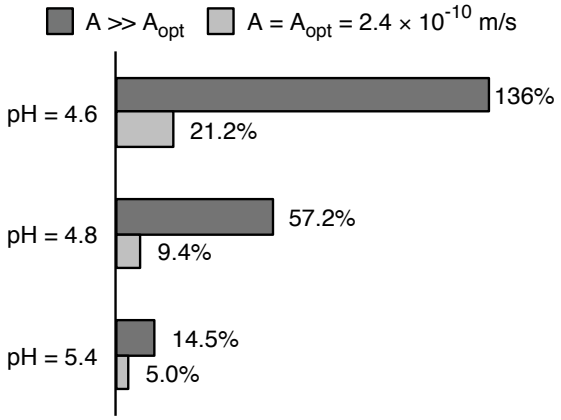

Fig. 4: Simulation MAPE_{exp} values for the cases of diffusion-controlled transfer resistance ($A \gg A_{\text{opt}}$) and mixed reaction-diffusion resistance ($A = A_{\text{opt}} = 2.4 \times 10^{-10}$ m/s) for the experimental data of Ciceri et al. (2011b). MAPE_{exp} is defined in Eq. 20

rate decreases the contribution of kinetic transfer resistance relative to diffusional resistance

To clarify effects of the buffer on the extraction regime, *MEDUSA* software (Puigdomenech 2009) was used to generate a speciation diagram (not presented) for the system. Within the present experimental pH range, it was shown that the fraction of cobalt-acetate complexes was approximately between 40–60%. The formation of these complexes, which has been neglected in the mechanism, only acts to increase the reaction rate (Simonin et al. 2003; Wasan et al. 1984). As a consequence, a mixed reaction-diffusion transport regime would still be concluded.

4.4 Results at higher extractant concentration

Simulation results for the new experimental data of the present study are shown in Table 6. As per Section 4.3, the simulations were undertaken for both diffusion-controlled and mixed reaction-diffusion controlled conditions. The same value of A_{opt} as that obtained in Section 4.2 was used. Figure 5 shows the values of MAPE_{exp} for all cases considered. The value of MAPE_{exp} for the case $[(\text{HL})_2]_0 = 10$ mM has been based on a summation over all data in Table 5. For low initial concentrations of the DEHPA extractant, the mixed reaction-diffusion simulations gave lower MAPE_{exp} values than the corresponding diffusion-controlled sim-

ulations. For the higher inlet concentration of, $[(HL)_2]_0 = 51$ mM, *both* simulation cases resulted in a $MAPE_{exp}$ value of order 50%. The effect of higher DEHPA concentration is also shown in the parity plots of Figure 6. For the simulations at low inlet DEHPA concentration (Figure 6a) the simulation and experimental values agree within the error bounds. At higher DEHPA concentrations (Figure 6b) the simulation consistently underestimates the experimental value. This deviation is attributed to a change in the extraction mechanism and/or physical properties. At high concentrations large Co-DEHPA polymers are formed (Kolařík and Grimm 1976; Yu et al. 1998). The formation of these polymeric species does not necessarily follow the reaction path of Eq. 5 and Eq. 6 and the rate law (Eq. 14) may change. The equilibrium constant determined in this study (Figure 1), as well as the physical properties shown in Table 3, are not valid upon the formation of polymeric species in the extraction system. Additional model parameters need to be accounted for if modelling of mass transfer in concentrated systems is envisaged.

Table 5: Outlet $CoL_2(HL)_2$ concentrations $\bar{c}$ (mM) for the corresponding experimental data of Ciceri et al. (2011b), $[Co^{II}]_0 = 5$ mM, $[(HL)_2]_0 = 10$ mM: (a) pH = 4.6, (b) pH = 4.8, (c) pH = 5.4

	Quantity	Flow rate (mL/hr) and outlet concentration (mM)					
(a)	F_{org} (mL/hr)	1.89	1.18	0.98	0.69	0.46	0.39
	F_{aq} (mL/hr)	2.02	0.84	0.64	0.45	0.40	0.25
	$\bar{c}_{exp}$	0.080 ± 0.005	0.19 ± 0.02	0.23 ± 0.05	0.250 ± 0.009	0.32 ± 0.07	0.36 ± 0.02
	$\bar{c}_{A \gg A_{opt}}$ [a]	0.32	0.38	0.41	0.50	0.64	0.67
	$\bar{c}_{A_{opt}}$	0.14	0.19	0.21	0.28	0.38	0.41
(b)	F_{org} (mL/hr)	2.08	1.01	0.66	0.52	0.41	
	F_{aq} (mL/hr)	1.90	0.99	0.73	0.51	0.43	
	$\bar{c}_{exp}$	0.220 ± 0.003	0.31 ± 0.02	0.39 ± 0.05	0.60 ± 0.1	0.66 ± 0.04	
	$\bar{c}_{A \gg A_{opt}}$	0.37	0.54	0.69	0.76	0.87	
	$\bar{c}_{A_{opt}}$	0.20	0.33	0.45	0.52	0.61	
(c)	F_{org} (mL/hr)	1.99	1.01	0.72	0.50	0.38	
	F_{aq} (mL/hr)	2.01	0.98	0.72	0.53	0.40	
	$\bar{c}_{exp}$	0.420 ± 0.006	0.64 ± 0.06	0.80 ± 0.09	1.0 ± 0.2	1.3 ± 0.3	
	$\bar{c}_{A \gg A_{opt}}$	0.53	0.74	0.89	1.08	1.25	
	$\bar{c}_{A_{opt}}$	0.43	0.63	0.77	0.96	1.11	

[a] $\bar{c}_{A \gg A_{opt}}$ denotes the simulation outlet concentration result using $A \gg A_{opt}$

Table 6: Outlet $CoL_2(HL)_2$ concentrations $\bar{c}$ (mM) of all models for present experimental data, $[Co^{II}]_0 = 5\,mM$, pH = 4.8: (a) $[(HL)_2]_0 = 5\,mM$, (b) $[(HL)_2]_0 = 51\,mM$

	Quantity	Flow rate (mL/hr) and outlet concentration (mM)					
(a)	F_{org} (mL/hr)	2.06	0.98	0.70	0.47	0.38	0.31
	F_{aq} (mL/hr)	1.96	1.02	0.67	0.54	0.40	0.33
	$\bar{c}_{exp}$	0.09 ± 0.02	0.18 ± 0.03	0.19 ± 0.03	0.3 ± 0.2	0.30 ± 0.09	0.29 ± 0.04
	$\bar{c}_{A \gg A_{opt}}$	0.17	0.25	0.30	0.38	0.42	0.46
	$\bar{c}_{A_{opt}}$	0.08	0.13	0.17	0.23	0.26	0.30
(b)	F_{org} (mL/hr)	2.06	0.98	0.68	0.47	0.38	0.30
	F_{aq} (mL/hr)	1.96	1.02	0.74	0.52	0.41	0.32
	$\bar{c}_{exp}$	1.6 ± 0.2	2.4 ± 0.2	3.0 ± 0.3	3.2 ± 0.2	3.4 ± 0.5	3.7 ± 0.1
	$\bar{c}_{A \gg A_{opt}}$	0.74	1.12	1.38	1.69	1.87	2.11
	$\bar{c}_{A_{opt}}$	0.71	1.07	1.31	1.60	1.79	2.07

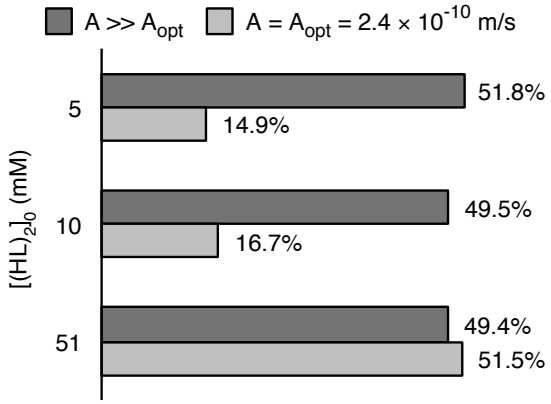

Fig. 5: $MAPE_{exp}$ values for the cases of diffusion-controlled transfer resistance ($A \gg A_{opt}$) and mixed reaction-diffusion resistance ($A = A_{opt} = 2.4 \times 10^{-10}$ m/s) for all experimental data considered. $MAPE_{exp}$ is defined in Eq. 20

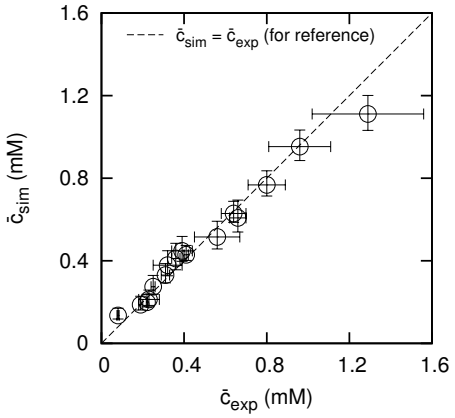

(a) $[(\mathrm{HL})_2]_0 = 10\,\mathrm{mM}$

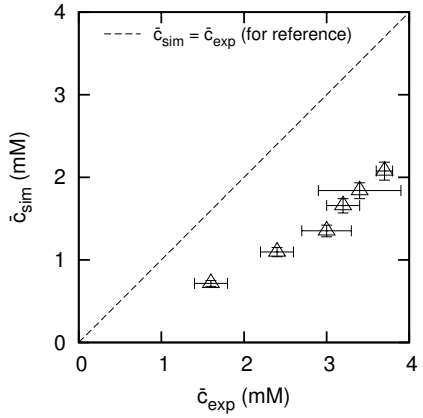

(b) $[(\mathrm{HL})_2]_0 = 51\,\mathrm{mM}$

Fig. 6: Parity plots demonstrating failure of mixed reaction-diffusion controlled simulations to predict experimental data at higher values of $[(\mathrm{HL})_2]_0$: (a) experimental data of Ciceri et al. (2011b) from Table 5, (b) experimental data from Table 6b

5 Conclusion

Finite volume CFD simulations were used to model experimental μSX data for Co^{II} extraction by di-(2-ethylhexyl) phosphoric acid (DEHPA). The reaction was shown to occur under a mixed reaction-diffusion transfer resistance regime. The device-independent reaction rate constant for this buffered system was determined to be $A = (2.4 \pm 0.6) \times 10^{-10}$ m/s based on the two-step interfacial mechanism of Komasawa and Otake (1983). The value is in good agreement with the corresponding Lewis cell measurement of $k_2K_1 = 1.8 \times 10^{-10}$ m/s (Komasawa and Otake 1983). Use of μSX takes advantage of the inherent characteristics associated with the micro scale including high specific interfacial areas, small quantities of chemicals, laminar flow conditions and the potential to investigate high species concentration regimes. This study has demonstrated the use of μSX in characterising the kinetics of a hydrometallurgical extraction process.

Acknowledgements Support from the Australian Research Council and the Particulate Fluids Processing Centre is gratefully acknowledged.

References

Albery WJ, Burke JF, Leffler EB, Hadgraft J (1976) Interfacial transfer studied with a rotating diffusion cell. J Chem Soc Faraday T 1 72:1618–1626

Aota A, Mawatari K, Kitamori R (2009) Parallel multiphase microflows: fundamental physics, stabilization methods and applications. Lab Chip 9:2470–2476

Beneitez P, Ortiz SJ, Ortega J (1985) Influence of the acetate medium on the extraction of cobalt (II) by di-2-ethylhexyl phosphoric acid. Solvent Extr Ion Exc 3(5):667–678

Biswas RK, Banu RA, Islam MN (2003) Some physico-chemical properties of D2EHPA. Part 2. Distribution, dimerization and acid dissociation constants in *n*-hexane/1 M $(Na^+,H^+)SO_4^{2-}$ system, interfacial adsorption and excess properties. Hydrometallurgy 69(1-3):157–168

Brisk ML, McManamey WJ (1969) Liquid extraction of metals from sulphate solutions by alkylphosphoric acids. I. Equilibrium distributions of copper, cobalt and nickel with di-(2-ethyl hexyl) phosphoric acid. J Appl Chem 19(4):103–108

Cianetti C, Danesi PR (1983) Kinetics and mechanism of the interfacial mass transfer of Zn^{2+}, Co^{2+}, Ni^{2+} in the system: bis (2-ethylhexyl) phosphoric acid, *n*-dodecane – KNO_3, water. Solvent Extr Ion Exc 1(1):9–26

Ciceri D, Perera JM, Stevens GW (2011a) A study of molecular diffusion across a water/oil interface in a Y-Y shaped microfluidic device. Microfluid Nanofluid 11(5):593–600

Ciceri D, Perera JM, Stevens GW (2011b) Extraction of Co(II) by di (2-ethylhexyl) phosphoric acid in a microfluidic device. In: Int Solvent Extr Conf (ISEC 2011), Santiago, Chile, ISEC, Santiago, Chile, p 112

Cotton FA, Wilkinson G (1988) Advanced Inorganic Chemistry, 5th edn. John Wiley & Sons, Inc.

Danesi PR, Vandegrift GF (1981) Activity coefficients of bis (2-ethylhexyl) phosphoric acid in n-dodecane. Inorg Nucl Chem Lett 17:109–115

Danesi PR, Reichley-Yinger L, Mason G, Kaplan L, Horwltz EP, Diamond H (1985) Selectivity-structure trends in the extraction of Co(II) and Ni(II) by dialkyl phosphoric, alkylphosphonic, and dialkylphosphinic acids. Solvent Extr Ion Exc 3(4):435–452

Dreisinger DB, Cooper WC (1986) The kinetics of cobalt and nickel extraction using HEHEHP. Solvent Extr Ion Exc 4:317–344

Dreisinger DB, Cooper WC (1989) The kinetics of zinc, cobalt and nickel extraction in the D2EHPA-heptane-HC104 system using the rotating diffusion cell technique. Solvent Extr Ion Exc 7(2):335–360

Eigen M (1963) Fast elementary steps in chemical reaction mechanisms. Pure Appl Chem 6:97–115

Flett DS (2005) Solvent extraction in hydrometallurgy: the role of organophosphorus extractants. J Organomet Chem 690(10):2426–2438

Golding JA, Pushparajah (1985) Mass transfer characteristics of cobalt and nickel in di(2-ethylhexyl)phosphoric acid under steady-state extraction conditions. Hydrometallurgy 14(3):295–307

Golding JA, Fouda SA, Saleh V (1977) Equilibrium and mass transfer for the separation of nickel and cobalt in di(2-ethylhexyl) phosphoric acid. In: International Solvent Extraction Conference (ISEC 1977), Toronto, Canada, pp 227–232

Golding JM, Saleh VM (1980) Mass transfer coefficient in di(2-ethylhexyl)phopshoric acid for cobalt and nickel. In: International Solvent-Extraction Conference (ISEC 1980), University of Liege, Belgium, vol 1, pp 80–194

Grimm R, Kolařík Z (1974) Acidic organophosphorus extractants–XIX: Extraction of Cu(II), Ni(II), Zn(II) and Cd(II) by di (2-ethylhexyl) phosphoric acid. J Inorg Nucl Chem 36(1):189–192

Harvie DJE (2012) An implicit finite volume method for arbitrary transport equations. ANZIAM J 52:C1126–C1145

Hotokezaka H, Tokeshi M, Harada M, Kitamori T, Ikeda Y (2005) Development of the innovative nuclide separation system for high-level radioactive waste using microchannel chip-extraction behavior of metal ions from aqueous phase to organic phase in microchannel. Prog Nucl Energ 47(1–4):439–447

Huang TC, Tsai TH (1990) Extraction equilibrium of cobalt (II) from sulphate solutions by di (2-ethylhexyl) phosphoric acid dissolved in kerosene. Polyhedron 9(9):1147–1153

Hughes M, Zhu T (1985) Rates of extraction of cobalt from an aqueous solution to D2EHPA in a growing drop cell. Hydrometallurgy 13:249–264

Juang RS, Jiang JD (1994) Rate-controlling mechanism of cobalt transport through supported liquid membranes containing di(2-ethylhexyl) phophoric acid. Separ Sci Technol 29(2):223–237

Kim HB, Ueno K, Chiba M, Kogi O, Kitamura N (2000) Spatially-resolved fluorescence spectroscopic study on liquid/liquid extraction processes in polymer microchannels. Anal Sci 16(8):871–876

Kolařík Z, Grimm R (1976) Acidic organophosphorus extractants—XXIV: The polymerization behaviour of Cu(II), Cd(II), Zn(II) and Co(II) complexes of di(2-ethylhexyl) phosphoric acid in fully loaded organic

phases. J Inorg Nucl Chem 38(9):1721 – 1727

Komasawa I, Otake T (1983) Kinetic studies of the extraction of divalent metals from nitrate media with bis(2-ethylhexyl)phosphoric acid. Ind Eng Chem Fund 22(4):367–371

Komasawa I, Otake T, Higaki Y (1981) Equilibrium studies of the extraction of divalent metals from nitrate media with di-(2ethylhexyl) phosphoric acid. J Inorg Nucl Chem 43(12):3351–3356

Kuban J, Dasgupta P, Berg PK (2003) Vertically stratified flows in microchannels. Computational simulations and applications to solvent extraction and ion exchange. Anal Chem 75(14):3549–3556

Lewis JB (1954a) The mechanism of mass transfer of solutes across liquid-liquid interfaces. 1. The determination of individual transfer coefficients for binary systems. Chem Eng Sci 3(6):248–259

Lewis JB (1954b) The mechanism of mass transfer of solutes across liquid-liquid interfaces. 2. The transfer of organic solutes between solvent and aqueous phases. Chem Eng Sci 3(6):260–278

Lo TC, Baird MHI, Hanson C (1983) Handbook of solvent extraction. Wiley, New York

MacLean D, Dreisinger D (1993) The kinetics of zinc extraction in the di(2-ethylhexyl) phosphoric acid, n-heptane-Zn(ClO4)2, HClO4, H2O system using the rotating diffusion cell. Hydrometallurgy 33(1-2):107 – 136

Maruyama T, Matsushita H, Uchida J, Kubota F, Kamiya N, Goto M (2004) Liquid membrane operations in a microfluidic device for selective separation of metal ions. Anal Chem 76:4495–4500

Mason LR, Ciceri D, Harvie DJE, Perera JM, Stevens GW (2012) Modelling of interfacial mass transfer in microfluidic solvent extraction. Part I. Heterogeneous transport. Microfluid Nanofluid Submitted

McCulloch JK, Perera JM, Kelly ED, White LR, Stevens GW, Grieser F (1996) A kinetic study of copper ion extraction by Kelex 100 at a heptane-water interface. J Colloid Interf Sci 184(2):406–413

Morita K, Hagiawara T, Hirayama N, Imura H (2010) Extraction of Cu(II) with dioctyldithiocarbamate and a kinetic study of the extraction using a two-phase microflow system. Solvent Extr Res Dev 17:209–214

Nagai H, Miwa N, Segawa M, Wakida S, Chayama K (2009) Quantification of Ag(I) and kinetic analysis using ion-pair extraction across a liquid/liquid interface in a laminar flow by fluorescence microscopy. J Appl Phys 105:102,015

Nichols KP, Pompano RR, Li L, Gelis AV, Ismagilov RF (2011) Toward mechanistic understanding of nuclear reprocessing chemistries by quantifying lanthanide solvent extraction kinetics via microfluidics with constant interfacial area and rapid mixing. JACS 133(39):15,721–15,729

Nishi K, Perera JM, Misumi R, Kaminoyama M, Stevens GW (2010) Study of diffusion of Co(II) and Co(II)-DEHPA complex in a microfluidic device. J Chem Eng Jpn 43(4):342–348

Nishi K, Perera JM, Misumi R, Kaminoyama M, Stevens GW (2011) Flow and diffusion behaviour as a function of viscosity in a double-Y-type microfluidic device. J Chem Eng Jpn 44(7):509–517

Perera JM, Stevens GW (2009) Spectroscopic studies of molecular interaction at the liquid-liquid interface. Anal Bioanal Chem 395(4):1019–1032

Perry RH, Green DW (2007) Perry's Chemical Engineers' Handbook, 8th edn. McGraw-Hill, New York

Priest C, Zhou J, Sedev R, Ralston J, Aota A, Mawatari K, Kitamori T (2011) Microfluidic extraction of copper from particle-laden solutions. Int J Miner Process 98(3-4):168 – 173

Puigdomenech I (2009) MEDUSA: (Make Equilibrium Diagrams Using Sophisticated Algorithms) program Inorganic Chemistry, Royal Institute of Technology, Stockholm, URL http://www.kemi.kth.se/medusa

Rydberg J (1969) Solvent extraction studies by the AKUFVE method. Part 1. Principle and general problems. Acta Chem Scand

Sella C, Bauer D (1988) Diphasic acido-basic properties of organophosphorus acids. Solvent Extr Ion Exc 6(5):819–833

Simonin JP (1996) A new version of the rotating stabilized cell technique for the study of extraction kinetics at a liquid-liquid boundary. Solvent Extr Ion Exc 14(5):889–896

Simonin JP, Turq P, Musikas C (1991) Rotating stabilised cell: a new tool for the investigation of interfacial extraction kinetics between liquid phases. J Chem Soc Faraday T 87:2715–2721

Simonin JP, Hendrawan H, Dardoize F, Clodic G (2003) Study of salt effects on the kinetics of extraction of cobalt(II) and zinc(II) at trace level by D2EHPA in *n*-dodecane. Hydrometallurgy 69(1-3):23–38

Stevens GW, Perera JM, Grieser F (2001) Interfacial aspects of metal ion extraction in liquid-liquid systems. Rev Chem Eng 17(2):87–210

Tokeshi M, Minagawa T, Kitamori T (2000) Integration of a microextraction system on a glass chip: Ion-pair solvent extraction of Fe(II) with 4,7-diphenyl-1,10-phenanthrolinedisulfonic acid and tri-*n*-octylmethylammonium chloride. Anal Chem 72(7):1711–1714

Van de Voorde I, Pinoy L, Courtijn E, Verpoort F (2005) Influence of acetate ions and the role of the diluents on the extraction of copper (II), nickel (II), cobalt (II), magnesium (II) and iron (II, III) with different types of extractants. Hydrometallurgy 78(1–2):92–106

de Voorde IV, Pinoy L, Courtijn E, Verpoort F (2006) Equilibrium Studies of Nickel(II), Copper(II), and Cobalt(II) Extraction with Aloxime 800, D2EHPA, and Cyanex Reagents. Solvent Extr Ion Exc 24(6):893–914

Žnidaršič-Plazl P, Plazl I (2009) Modelling and experimental studies on lipase-catalyzed isoamyl acetate synthesis in a microreactor. Process Biochem 44:1115–1121

Warren DB, Grieser F, Perera JM, Stevens GW (2006) Effect of surfactants on the kinetics of nickel(II) extraction by 2-hydroxy-5-nonylacetophenone oxime (LIX 84) in an n-heptane/water system. Langmuir 22(1):213–218

Wasan DT, Zhongmao MG, Li NN (1984) Separation of metal ions by ligand-accelerated transfer through liquid surfactant membranes. Faraday Symp Chem S 77:67–74

Wilke CR, Chang P (1955) Correlation of diffusion coefficients in dilute solutions. AIChE J 1(2):264–270

Yaws CL (2003) Yaws' Handbook of Thermodynamic and Physical Properties of Chemical Compounds. Knovel

Yu ZJ, Ibrahim TH, Neuman RD (1998) Aggregation behavior of cobalt(II), nickel(II), and copper(II) bis(2-ethylhexyl)phosphate complexes in *n*-heptane. Solvent Extr Ion Exc 16(6)

List of symbols

A	kinetic rate constant, (m/s)
Bo	Bond number ($Bo = \Delta\rho g D_\mathrm{h}^2/\gamma$), (–)
c	local species concentration, (mM)

$\mathscr{D}$	diffusivity, (m^2/s)
D_h	hydraulic diameter of microchannel half-volume, (m)
F	volumetric flow rate, (m^3/s)
g	gravitational acceleration, (m/s^2)
I	total initial ionic strength, (mM)
k_1, k_{-1}, k_2	interfacial reaction rate constants, (m/s)
k_f, k_b	forwards/backwards reaction rate constant
K_2	dimerisation constant ($[(HL)_2]_{org}/[(HL)]^2_{org}$), ($mM^{-1}$)
K_d	distribution constant ($[(HL)]_{org}/[(HL)]_{aq}$), (–)
K_{eq}	equilibrium constant, (–)
$MAPE_{exp}$	mean absolute percentage error (experimental reference), (–)
R	extraction rate per unit area, (mol/m^2 s)
RSS	residual sum of squares, (mol^3/m^6)
$\mathbf{u}$	fluid velocity, (m/s)
V_N	molar volume of solute at normal boiling point, (m^3/kmol)
x, y, z	Cartesian coordinates, (m)

Greek letters

γ	interfacial tension, (N/m)
ε	molar absorptivity, ($M^{-1}\,cm^{-1}$)
ρ	fluid density, (kg/m^3)
μ	dynamic viscosity, (Pa s)
ν	stoichiometric coefficient, (–)

Subscripts

0	initial
aq	aqueous phase
exp	experiment
i	ith phase
int	interface
j	jth species
org	organic phase

sim	simulation

Abbreviations

Ac^-	acetate
AcH	acetic acid
CFD	Computational Fluid Dynamics
DEHPA	di-(2-ethylhexyl) phosphoric acid
DHBA	2,2′-dihydroazobenzene
HL	condensed notation for DEHPA
$(HL)_2$	condensed notation for the dimeric form of DEHPA
HTCO	1,4,7,10,13,16-hexathiacyclooctadecane
Kelex 100	7-(4-ethyl-1-methyloctyl)-8-hydroxyquinoline
L^-	condensed notation for the deprotonated form of DEHPA
LIX 84	2-hydroxy-5-nonylacetophenone oxime
MAPE	Mean Absolute Percentage Error
MTWCR	Mass Transfer with Chemical Reaction
PC-88A	2-ethylhexyl phosphonic acid mono 2-ethylhexyl ester
TBP	tri-*n*-butylphosphate
SX	Solvent Extraction
μSX	Microfluidic Solvent Extraction